

Research Articles: Behavioral/Cognitive

Human lateral Frontal Pole contributes to control over emotional approach-avoidance actions

<https://doi.org/10.1523/JNEUROSCI.2048-19.2020>

Cite as: J. Neurosci 2020; 10.1523/JNEUROSCI.2048-19.2020

Received: 19 August 2019

Revised: 17 January 2020

Accepted: 17 January 2020

This Early Release article has been peer-reviewed and accepted, but has not been through the composition and copyediting processes. The final version may differ slightly in style or formatting and will contain links to any extended data.

Alerts: Sign up at www.jneurosci.org/alerts to receive customized email alerts when the fully formatted version of this article is published.

Human lateral Frontal Pole contributes to control over emotional approach-avoidance actions

Abbreviated title: FPI in emotional control

Bob Bramson¹, Davide Folloni^{3,4}, Lennart Verhagen^{3,4}, Bart Hartogsveld⁵, Rogier B. Mars^{1,4}, Ivan Toni^{1,*} and Karin
Roelofs^{1,2,*}

¹Donders Institute for Brain, Cognition and Behavior, Centre for Cognitive Neuroimaging, Radboud University
Nijmegen, 6525 EN Nijmegen, The Netherlands

²Behavioral Science Institute (BSI), Radboud University Nijmegen, 6525 HR Nijmegen, The Netherlands

³Wellcome Centre for Integrative Neuroimaging (WIN), Department of Experimental Psychology, University of
Oxford, Oxford, OX1 3SR, United Kingdom

⁴Wellcome Centre for Integrative Neuroimaging (WIN), Centre for Functional MRI of the Brain (FMRIB), Nuffield
Department of Clinical Neurosciences, John Radcliffe Hospital, University of Oxford, Oxford, OX3 9DU, United
Kingdom

⁵Department of Clinical Psychological Science, Faculty of Psychology and Neuroscience, Maastricht University,
6229 ER Maastricht, The Netherlands

* These authors contributed equally

Conflicts declared: none.

Number of pages: 34

Number of figures: 3

Words abstract: 232

Words introduction: 650

Words discussion: 1499

Correspondence:

Bob Bramson

Donders Centre for Cognitive Neuroimaging

Radboud University Nijmegen

Trigon Building

Kapittelweg 29

6525 EN Nijmegen

The Netherlands

E-mail: b.bramson@donders.ru.nl

Acknowledgements: This work was supported by a VICI grant (#453-12-001) from the Netherlands Organization
for Scientific Research (NWO) and a consolidator grant from the European Research Council (ERC_CoG-
2017_772337) awarded to Karin Roelofs. The work of RBM is supported by the Netherlands Organization for
Scientific Research (NWO) [452-13-015]. The work of DF was supported by Wellcome Trust UK Grant
(105238/Z/14/Z).

38 **Abstract**

39 Regulation of emotional behavior is essential for human social interactions. Recent work has
40 exposed its cognitive complexity, as well as its unexpected reliance on portions of the anterior
41 prefrontal cortex (aPFC) also involved in exploration, relational reasoning, and counterfactual choice,
42 rather than on dorsolateral and medial prefrontal areas involved in several forms of cognitive
43 control. This study anatomically qualifies the contribution of aPFC territories to the regulation of
44 prepotent approach-avoidance action-tendencies elicited by emotional faces, and explores a possible
45 structural pathway through which this emotional action regulation might be implemented.

46 We provide converging evidence from task-based fMRI, diffusion-weighted imaging, and
47 functional connectivity fingerprints for a novel neural element in emotional regulation. Task-based
48 fMRI in human male participants (N = 40) performing an emotional approach-avoidance task
49 identified aPFC territories involved in the regulation of action-tendencies elicited by emotional faces.
50 Connectivity fingerprints, based on diffusion-weighted imaging and resting-state connectivity,
51 localized those task-defined frontal regions to the lateral frontal pole (FPI), an anatomically-defined
52 portion of the aPFC that lacks a homologous counterpart in macaque brains. Probabilistic
53 tractography indicated that 10-20% of inter-individual variation in emotional regulation abilities is
54 accounted for by the strength of structural connectivity between FPI and amygdala. Evidence from an
55 independent replication sample (N = 50; 10 females) further substantiated this result. These findings
56 provide novel neuroanatomical evidence for incorporating FPI in models of control over human
57 action-tendencies elicited by emotional faces.

58

59

60 **Keywords:** social-emotional action control, amygdalofugal connectivity, prefrontal control, approach-
61 avoidance, lateral frontal pole

62 **Significance statement**

63 Successful regulation of emotional behaviors is a prerequisite for successful participation in
64 human society, as is evidenced by the social isolation and loss of occupational opportunities often
65 encountered by people suffering from emotion-regulation disorders such as social-anxiety disorder
66 and psychopathy. Knowledge about the precise cortical regions and connections supporting this
67 control is crucial for understanding both the nature of computations needed to successfully traverse
68 the space of possible actions in social situations, and the potential interventions that might result in
69 efficient treatment of social-emotional disorders. This study provides evidence for a precise cortical
70 region (FPI) and a structural pathway (the ventral amygdalofugal bundle) through which a cognitively
71 complex form of emotional action regulation might be implemented in the human brain.

72

73

74

75

76

77

78

79

80

81

82

83 **Introduction**

84 Control over emotional behavior is paramount for successful participation in society (Hare,
 85 2017). However, regulating emotional actions is cognitively complex. It requires the ability to assess
 86 the effectiveness of on-going behavior and compare this with alternative action strategies. For
 87 instance, a scientist presenting their work in front of a critical audience needs to overcome the
 88 tendency to avoid potential criticism in order to reap the long-term benefits of peer-exposure and
 89 constructive feedback. Recent converging evidence indicates that this type of regulation of emotional
 90 behavior is implemented by the rostral part of the anterior prefrontal cortex (aPFC; Volman et al.
 91 2011, 2013; Koch et al. 2018). The current study anatomically qualifies the contribution of aPFC
 92 regions to the regulation of emotional action-tendencies elicited by social-emotional cues, and
 93 explores a structural pathway through which this regulation might be implemented.

94 The aPFC has been involved in a disparate range of cognitive tasks, e.g. relational reasoning
 95 (Vendetti and Bunge, 2014; Hartogsveld et al., 2017), counterfactual choice (Boorman et al., 2009a;
 96 Mansouri et al., 2017), exploration behavior (Daw et al., 2006; Zajkowski et al., 2017). To date,
 97 emotional action regulation has not been considered part of the cognitive fingerprint of this region
 98 (Koch et al., 2018). Models of emotion-regulation have predominantly focused on dorsolateral and
 99 medial prefrontal cortex (mPFC; Etkin et al., 2015; Morawetz et al., 2017; Langner et al., 2018). These
 100 models are largely based on explicit regulation strategies (e.g. reappraisal; Wager et al., 2008; Buhle
 101 et al., 2014) and have ignored control of emotional actions, an important component of emotion-
 102 regulation concerned with conflict between the emotional value of stimulus and response (Frijda et
 103 al., 2014; Ridderinkhof, 2017; Bramson et al., 2018). At first glance, the focus of the emotion control
 104 literature on mPFC is justified by strong structural and functional connectivity between mPFC and
 105 areas involved in emotional and social processing, such as the amygdala (Ghashghaei and Barbas
 106 2002; Petrides and Pandya 2007; Neubert et al. 2014; Tillman et al. 2018). In contrast, structural
 107 connections to the amygdala are scarce for anterior prefrontal areas (Ghashghaei et al., 2007).

108 However, recent studies have shown that the amygdala is connected to the aPFC via rostral
 109 projections of the ventral amygdalofugal pathway (Krüger et al., 2015; Kamali et al., 2016). In fact,
 110 there is evidence that this tract might extend to the lateral frontal pole (FPI; Folloni et al., 2019), a
 111 portion of the human aPFC that does not have a homological counterpart in macaque brains
 112 (Neubert et al., 2014). These anatomical observations, together with converging functional evidence
 113 on aPFC involvement in the regulation of emotional strategies and actions (Bramson et al., 2018;
 114 Koch et al., 2018) raise the possibility that human emotional action control is coordinated by the FPI.

115 In this study, we combine evidence from task-based fMRI, diffusion-weighted imaging, and
 116 resting-state connectivity fingerprints to define which portion of aPFC supports emotional action
 117 control. First, we characterize the functional specificity of aPFC contributions to emotional action
 118 control through a social-emotional approach-avoidance (AA) task. Participants approached or
 119 avoided happy and angry faces by means of speeded joystick reactions. Approaching angry and
 120 avoiding happy faces requires control over habitual emotional action-tendencies, and elicits activity
 121 in aPFC (Roelofs et al., 2008; Volman et al., 2011b). The social relevance of the emotional-control
 122 indexed by this task has been established in social-emotional disorders (Bertsch et al., 2017; Volman
 123 2016) and healthy individuals where it predicted responses to real-life social stress-induction
 124 (Kaldewaij et al., 2019a). Second, we anatomically localize aPFC territories activated by the approach-
 125 avoidance task by matching structural and functional connectivity fingerprints of this area to
 126 fingerprints extracted from known areas of the aPFC (Neubert et al. 2014). Third, we assess the
 127 evidence for and the functional relevance of a structural pathway through which the portion of the
 128 aPFC activated by the AA task might support emotional action regulation, namely through direct
 129 connections with the amygdala (Folloni et al., 2019).

130 **Methods**

131 *Participants*

Forty male students from the Radboud University Nijmegen participated in this study after giving informed consent. The sample had a mean age of 23.5 years (sd: 2.8, range 18-33 years). None of the participants reported history of mental illness or use of psychoactive/corticosteroid medication. All had normal or corrected to normal vision, and were screened for counter indications for magnetic resonance imaging (MRI). The study was approved by the local ethics committee (CMO:2014/288). Sample size was based on behavioral congruency effects observed previously in the same task (effect size $d = .4$; Volman et al, 2011). The sample consisted of males only in order to minimize potential variability caused by sex differences and fluctuations in cortisol and testosterone (e.g. due to different phases in the menstrual cycle). These hormones are known to influence behavioral and neural responses on the AA task (van Peer et al., 2007; Volman et al., 2011b; Kaldewaij et al., 2019a) and controlling for those fluctuations would have required a larger sample.

Given the novelty of one of the main findings of this report (correlation between amygdalofugal-FPI connectivity and behavioral congruency effect – see Results), we set out to replicate that finding in an independent convenience sample consisting of 50 participants [10 females, mean age = 23.8 (sd = 3.4, range 18-34)]. These participants took part in another study where they performed the AA task in a similar test-context, as well as a Diffusion weighted imaging (DWI) session. This second study was performed as part of a larger research project, after the analyses of the current study were finalized.

Materials and apparatus

Images were acquired using a 3T MAGNETOM Prisma MRI scanner (Siemens AG, Healthcare Sector, Erlangen, Germany) using a 32 channel headcoil for functional and DWI images and a 20 channel headcoil for structural T1 images. Stimuli were presented using an EIKI LC- XL100 beamer with a resolution of 1024 x 768 and a refresh rate of 60 Hz, and were projected onto a screen behind the scanner bore. Participants were able to see the screen via a mirror.

156 The approach-avoidance (AA) task consisted of 16 blocks of 12 trials each, in which
 157 participants had to approach or avoid equiluminant happy or angry faces presented in the centre of
 158 the screen. Faces were presented for 100 ms and preceded by a 500 ms fixation cross in the centre of
 159 the screen. After the presentation of the face, participants had 2000 ms to respond using a joystick.
 160 Each trial was followed by an intertrial interval of 2 – 4 seconds. Task instructions for congruent
 161 (move the joystick towards you/away from you for happy/angry faces), and incongruent blocks
 162 (move the joystick towards you/away from you for angry/happy faces), were presented before each
 163 block and switched between blocks. Subjects responded using a customized fiber optic response
 164 joystick, which was fixed to only move in the sagittal plane. Affect-incongruent trials have
 165 consistently been shown to activate the aPFC (Roelofs et al. 2008; Volman et al. 2011; Tyborowska et
 166 al. 2016; Kaldewaij et al., 2019). Behavioral and neural responses on this task are affected in several
 167 social-emotional disorders such as psychopathy, social-anxiety and borderline disorder (Heuer et al.,
 168 2007; von Borries et al., 2012; Roelofs and Cremers, 2015; Bertsch et al., 2018), and those responses
 169 are influenced by hormones affecting social behavior (Volman et al., 2016; Kaldewaij et al., 2019a).

170 *Procedure*

171 Data were acquired on two different days; day one consisted of the AA task, resting-state and
 172 T1 structural scan. DWI was acquired on the second day. Before and after the AA task we took saliva
 173 measurements to possibly control for testosterone and cortisol for other research purposes. On the
 174 second day, each participant filled out the State Trait Anxiety Inventory to control for effects of trait
 175 anxiety.

176 *Functional scans*

177 The field of view of the scans acquired in the two MR-sessions was aligned to a built-in brain-
 178 atlas using an auto-align head scout sequence. During resting state and task fMRI sessions we
 179 acquired BOLD-sensitive images using a multiband sequence with TR = 735 ms/TE = 39ms, 64 slices,
 180 flip angle of 52°, multiband acceleration factor of 8, slice orientation T > C, voxel size = 2.4 x 2.4 x 2.4

181 mm, phase encoding direction A >> P. The resting state session lasted 8.5 minutes (700 images). Each
 182 sequence was followed by a field map image; flip angle = 60°, TR = 614, TE = 4.92.

183 *Structural scan*

184 High-resolution anatomical images were acquired with a single-shot MPAGE sequence with
 185 an acceleration factor of 2 (GRAPPA method), a TR of 2400 ms, TE 2.13 ms. Effective voxel size was 1
 186 x 1 x 1 mm with 176 sagittal slices, distance factor 50%, flip angle 8°, orientation A >> P, FoV 256 mm.

187 *DW imaging*

188 Diffusion-weighted images were acquired using echo-planar imaging with an acceleration
 189 factor of 2 (GRAPPA method). We acquired 65 2 mm-thick axial slices, with a voxel size of 2 x 2 x 2
 190 mm, phase encoding direction A >> P, FoV 220 mm. In addition, we acquired 10 volumes without
 191 diffusion weighting ($b = 0 \text{ s/mm}^2$), 30 isotropically distributed directions using a b-value of 750
 192 s/mm^2 , and 60 isotropically distributed directions a b-value of 3000 s/mm^2 . We also acquired a
 193 volume without diffusion weighting with reverse phase encoding (P >> A).

194 Diffusion-weighted images for the replication sample were acquired using echo-planar
 195 imaging with multiband acceleration factor of 2 (GRAPPA method), multiband acceleration factor = 3.
 196 For this dataset we acquired 93 1.6 mm thick transversal slices with voxel size of 1.6 x 1.6 x 1.6 mm,
 197 phase encoding direction A >> P, FoV 211 mm, TR = 3350, TE = 71.20. 256 isotropically distributed
 198 directions were acquired using a b-value of 2500 s/mm^2 . We also acquired a volume without
 199 diffusion weighting with reverse phase encoding (P >> A). Preprocessing and analyses for this dataset
 200 were the same as for the original sample (reported below).

201 *Behavioral analyses*

202 Behavioral analyses of AA task performance contrasted incongruent to congruent trials,
 203 comparing reaction times and percentage correct between conditions. Differences between

204 conditions were assessed using repeated measures ANOVA and paired-sample t-tests implemented
205 in JASP (version 0.9.2; <https://jasp-stats.org/>).

206 *Analyses - functional images*

207 All processing of the AA and resting state images was done using MELODIC 3.00 as
208 implemented in FSL 5.0.10 (<https://fsl.fmrib.ox.ac.uk>). Images were motion corrected using MCFLIRT
209 (Jenkinson et al., 2002), and distortions in the magnetic field were corrected using fieldmap
210 correction in FUGUE. Functional images were rigid-body registered to the brain extracted structural
211 image using FLIRT. Registration to MNI 2mm standard space was done using the nonlinear
212 registration tool FNIRT. Images were spatially smoothed using a Gaussian 5 mm kernel and low
213 passed filtered with a cut-off at 100 s. Independent component analysis was run (Beckmann and
214 Smith, 2004), after which the first 10 components were manually inspected to remove sources of
215 noise (Griffanti et al., 2017).

216 First and second level analyses were done in FEAT 6.00 implemented in FSL 5.0.10
217 (<https://fsl.fmrib.ox.ac.uk/fsl/fslwiki/>; Woolrich et al., 2001, 2004). We set up separate general linear
218 models for each task. The first-level AA model consisted of four task regressors: Approach angry,
219 approach happy, avoid angry and avoid happy; six motion regressors and their temporal derivatives;
220 and two regressors modeling fluctuations in signal in white matter and cerebrospinal fluid. Approach
221 happy and avoid angry (congruent conditions) were then contrasted with approach angry and avoid
222 happy (incongruent conditions). This contrast was taken as input for each subject in the second level
223 analysis. Second level analysis was performed using FMRIB's Local Analysis of Mixed Effects (FLAME
224 1) with outlier de-weighting. We used a cluster forming threshold of $Z > 2.3$, a value that has been
225 shown to effectively control for Family Wise Error rate, possibly related to the fact that FLAME
226 estimates and takes into account within subject variance (Eklund et al., 2015). Locations with above
227 threshold activity were localized using masks for the prefrontal cortex (Sallet et al., 2013; Neubert et

228 al., 2014), parietal cortex (Mars et al., 2011) and whole brain cortical and subcortical atlases
 229 (Harvard-Oxford atlas).

230 To assess psychophysiological interactions (PPI) during the AA task we ran a second analysis
 231 using FEAT with regressors representing the task effects of interest (incongruent-congruent), the
 232 regressor incongruent + congruent, a regressor describing the first eigenvariate time series of
 233 activation of the seed region: Bilateral amygdalae taken from the AAL atlas (Tzourio-Mazoyer et al.,
 234 2002), and a regressor describing the interaction between the seed region activity and task effects.
 235 Strength of amygdalofugal-FPI connections as estimated from tractography of dw-MRI (see below)
 236 was added as a covariate in the second level analysis.

237 *Analyses – functional connectivity fingerprints of FPI based on resting-state fMRI*

238 For the resting state fMRI analysis we defined regions-of-interest for each of the three areas
 239 in aPFC (FPI, FPM, and 46), as identified by Neubert et al. (2014). These masks were thresholded to
 240 contain only the 25% of voxels that were most likely to be part of each area (Mars et al., 2016;
 241 Hartogsveld et al., 2017). The masks were warped to each individual anatomical space, after which
 242 we extracted the first eigenvariate time series from each area. These time series were correlated
 243 with whole brain resting state activity, the results of which were transformed to z-values using
 244 Fishers z-transform and normalized. Resulting correlation maps were transformed back to MNI space
 245 after which we extracted the connectivity from each prefrontal region with five downstream regions:
 246 Posterior Cingulate Cortex (PCC) [10 -52 24], Intraparietal lobule (IPL) [48 -46 48], temporal pole (TP)
 247 [34 12 -36], ventromedial prefrontal cortex (vmPFC) [8 44 -14] and dorsolateral prefrontal cortex
 248 (dlPFC) [46 20 40], for each hemisphere separately. Differential connectivity with these five areas has
 249 previously been shown to be appropriate to dissociate different cortical regions within aPFC (Mars et
 250 al. 2016; Hartogsveld et al. 2017). This procedure creates a “connectivity fingerprint” of each region,
 251 describing functional (and structural for DWI analyses) connections with other brain areas, and rests
 252 on the premise that each regions’ unique functional repertoire is determined by its connections with

other regions (Passingham et al., 2002; Mars et al., 2018). We followed the same procedure for the two regions found in the aPFC during the AA task: 5 mm sphere around MNI [24 50 -4] and MNI [-24 52 4]. The focus of this study on aPFC responses to congruency demands during performance of the AA task is related to a large body of work that has characterized and replicated those aPFC responses across numerous studies (Roelofs et al., 2008; Volman et al., 2011a; Tyborowska et al., 2016). That work has shown that activity in aPFC during incongruent trials is correlated with and necessary for successfully overriding automatic action-tendencies (Volman et al., 2011a); is influenced by several neuromodulators such as testosterone and cortisol (van Peer et al., 2007; Volman et al., 2011b, 2016; Kaldewaij et al., 2019a); is augmented in social psychopathology (von Borries et al., 2012; Radke et al., 2013; Bertsch et al., 2017, 2018); and predicts real-world stress coping (Kaldewaij et al., 2019b). The added value and validity of the structural explanation provided in the current study depends on using the same functional comparison implemented in those previous studies, namely a direct contrast between incongruent and congruent conditions.

For the statistical analysis, we computed the “city block” or “Manhattan” distance between the connectivity profiles of the AA regions and the connectivity profiles of the three prefrontal masks, separately for each hemisphere. This measure consists of the sum of absolute distance between different connectivity profiles and has previously been used to describe the relative dissimilarity between different connectivity profiles (Sallet et al., 2013; Neubert et al., 2014; Mars et al., 2016). We compared these distance measures to a distribution of randomized distances that we created by permuting the region labels 10000 times, each time randomly swapping the target region labels (FPI; FPM; area 46) within participants and computing the Manhattan distance with the AA fingerprint. The result of this approach shows whether the connectivity profile of the aPFC regions differs from the connectivity profile of the region active during the AA task (Mars et al., 2016).

Analyses – structural connectivity fingerprints of FPL based on diffusion-weighted MRI

277 All analyses of diffusion data were performed in FSL FDT 3.0 (<https://fsl.fmrib.ox.ac.uk>). We
 278 used TOPUP to estimate susceptibility artifacts using additional $b = 0$ volumes with reverse phase
 279 coding direction (Andersson et al., 2003). Next, we used EDDY (using the fieldmap estimated by
 280 TOPUP) to correct for distortions caused by eddy currents and subject movement (Andersson and
 281 Sotiropoulos, 2016). We used BedpostX to fit a crossing fiber model using default settings (Behrens
 282 et al., 2007).

283 Seed regions were defined for five major tracts by creating 5 mm spheres in the Cingulum
 284 Bundle (CB) MNI: [8 -2 36], Superior Longitudinal Fasciculus 1 (SLF1), MNI: [16 -2 54], SLF 2, MNI: [30
 285 -2 38], SLF 3, MNI: [44 -2 26] and Uncinate Fasciculus, MNI: [32 -2 -10] and then warped to individual
 286 subject space. As with the functional connectivity described above, these specific fiber bundles were
 287 chosen because they have been shown to be differentially connected to distinct areas within the
 288 aPFC (Neubert et al., 2014; Mars et al., 2016; Hartogsveld et al., 2017). The procedure for
 289 Amygdalofugal connectivity is described below. For the comparisons in the left hemisphere the same
 290 coordinates were used with the x-axis coordinate inverted. ProbtrackX was run with default settings
 291 using these masks as seed, separately for each hemisphere using an exclusion mask at $x = 0$. The
 292 results from probtrackX were warped to MNI 1 mm space, log transformed, and normalized to the
 293 highest probability per tract to allow a direct comparison between tracts with all values ranging
 294 between 0 and 1. We computed connectivity profiles of FPI, FPM and area 46 by counting the
 295 number of times each tract ended in these regions. These connectivity profiles were compared to the
 296 connectivity profile of the region in the aPFC resulting from the AA task contrast (5 mm sphere at
 297 MNI: [24 50 -4] for right and MNI: [-24 52 4] for left). We computed Manhattan distance between the
 298 connectivity profiles of the AA task and the three prefrontal masks and permuted this 10,000 times,
 299 each time randomly swapping the target region labels (FPI; FPM; area 46) within participants.

300 *Analyses - Amygdalofugal connectivity*

301 Connections between amygdala and aPFC were reconstructed using probtrackX. For this we
 302 used the procedure and masks provided by Folloni et al., (2019). We seeded these connections in the
 303 white matter punctuating the extended amygdala and substantia innominata: MNI: [-7 3 -9] and an
 304 all-coronal waypoint mask at $y = 22$. We used tractography masks to ensure the estimated seedlines
 305 extended only rostrally, at least up to the $y = 25$ coronal plane, and excluded CSF and between-
 306 hemisphere connections. Connection strength was normalized and log transformed within each
 307 participant. Next we extracted the total amount of times the tractography entered the FPI, Fpm and
 308 area 46 regions-of-interest separately. These values were correlated with congruency effects on
 309 reaction time and percentage correct using Spearman's correlation coefficient.

310 To exclude that the Amygdalofugal-FPI connections are influenced by (much stronger)
 311 projections of the Uncinate Fasciculus (UF), we reconstructed UF connectivity with FPI and correlated
 312 this with the behavioral congruency. To isolate the UF we placed a seed in the white matter rostro-
 313 laterally to the amygdala (MNI: [35 2 -22]), a coronal waypoint mask at $y = 22$ and exclusion masks in
 314 the CSF and between hemispheres. We also used partial correlation to regress out possible
 315 correlations influences of UF and state anxiety (STAI-Y2) in the amygdalofugal-behavioral
 316 correlations. Finally, we used an independent comparison sample to confirm the correlation between
 317 amygdalofugal-FPI connectivity and behavioral congruency.

318 Results

319 The study had two main goals: i) localize aPFC responses evoked during control over action-
 320 tendencies elicited by emotional faces in relation to an established anatomical parcellation of the
 321 aPFC; and ii) provide evidence for the functional relevance of amygdala-aPFC connectivity in
 322 implementing control over emotional-actions. We implemented a-priori determined analyses
 323 addressing these two goals, correcting the statistical inferences for multiple comparisons, either
 324 through cluster correction (fMRI task contrasts), or Bonferroni-correction (anatomical localization
 325 and tract-behavioral correlations). Furthermore, we implemented a number of follow-up exploratory

326 analyses, prioritizing sensitivity over specificity, thus avoiding corrections for multiple comparisons.

327 The exploratory nature of these analyses is marked in the text.

328 *AA-task - Behavioral costs of controlling emotional behavior*

329 There were interaction effects between emotion and movement for reaction times; $F(1,39) =$
 330 26.5, $p < .001$ and error rates; $F(1,39) = 27.2$, $p < .001$. Reaction times were longer for incongruent (M
 331 = 673 ms, SD = 103) than for congruent movements (M = 626 ms, SD = 128), $t(39) = 5.12$, $p < .001$ with
 332 an effect size of $d = .4$, CI [.22 , 1.03], calculated as $(M1-M2) / sd_{pooled}$. Participants also made more
 333 errors during incongruent (M = 94.3 % correct, SD = 4.43) than congruent blocks (M = 97.1 % correct,
 334 SD = 2.96), $t(39) = 5.21$, $p < .001$; effect size $d = .7$, CI [.27 , 1.2]. In addition to these interaction
 335 effects there were main effects of movement $F(1,39) = 32.9$, $p < .001$; and emotion $F(1,39) = 7.7$, $p =$
 336 .008 on reaction times, but not on error rates, both $p > .15$. Approach movements were faster (M =
 337 626 ms, SD = 106) than avoid movements (M = 661 ms, SD = 111) and reactions to happy faces (M =
 338 635 ms, SD = 103) were faster than to angry faces (M = 652 ms, SD = 114). Interaction effects are
 339 depicted in figure 1B. These effects illustrate the behavioral cost of applying cognitive control over
 340 prepotent habitual emotional action-tendencies elicited by social-emotional stimuli.

341 In the replication sample there were similar interaction effects between emotion and
 342 movement for reaction times; $F(1,49) = 49.7$, $p < .001$ and error rates; $F(1,49) = 37.5$, $p < .001$.
 343 Reaction times were longer for incongruent (M = 676 ms, SD = 133) than congruent (M = 627 ms, SD
 344 = 107), $t(49) = 7$, $p < .001$; effect size $d = .4$, CI [.15 .97]. The replication sample also made more errors
 345 during incongruent (M = 94.5 % correct, SD = 3.8) than in congruent trials (M = 96.8 % correct, SD =
 346 2.9); $t(49) = 6.13$, $p < .001$, $d = .68$, CI [.11 1.25]. In addition to these effects of interest there were
 347 again main effects of movement $F(1,49) = 26.6$, $p < .001$ and emotion $F(1,49) = 7.5$, $p = .008$ on
 348 reaction times, but not on error rates, both $p > .23$. Approach movements were faster (M = 641 ms,
 349 SD = 122) than avoid movements (M = 661 ms, SD = 127) and reactions to happy faces (M = 645 ms,
 350 SD = 124) were faster than to angry faces (M = 657 ms, SD = 125).

351 *AA-task - Controlling emotional actions elicits frontal and parietal activation*

352 Building on previous evidence (Volman et al. 2011; Tyborowska et al. 2016), we expected
 353 that control over social emotional action-tendencies increases aPFC activity. This study tests whether
 354 this activity can be localized to the lateral Frontal Pole. We found clusters of increased activity over
 355 frontal areas during incongruent as compared to congruent trials, whole-brain cluster-level corrected
 356 for multiple comparisons (cluster-forming threshold of $Z > 2.3$ with corrected cluster threshold of $p <$
 357 $.05$). Overlaying the frontal activity profiles on the mask created by Neubert et al. (2014) confirmed
 358 activity in FPI, figure 1C. In addition we observed clusters of increased activity in bilateral
 359 intraparietal lobule, an area strongly connected to the aPFC (Mars et al., 2011); bilateral
 360 Insula/Inferior Frontal Gyrus [34 -26 -6]; Bilateral area 8A [40 6 42]; bilateral area 46 [30 50 16]; and
 361 bilateral cerebellum [16 -78 -30].

362 Contrasting happy and angry showed increased activity for happy trials in cerebellum [4 -62 -
 363 50], posterior cingulate [8 -48 24], anterior cingulate [-2 40 2] and lateral occipital cortex [30 -84 0].
 364 Avoid trials showed increased activity in Frontal orbital cortex [44 20 -10] and occipital cortex: [32 -
 365 66 54].

366 The estimated BOLD signal indexing control over emotional action-tendencies (incongruent
 367 vs congruent trials) extracted from FPI correlated positively with the behavioral index of emotional
 368 control (reaction time differences between incongruent and congruent trials): $r(38) = .33$, $p = .037$,
 369 figure 1D. This effect corroborates our earlier findings of a positive relationship between individual
 370 differences in reaction time effects and recruitment of aPFC/FPI activation (Roelofs et al. 2009;
 371 Bramson et al., 2018). Exploratory analyses correlating BOLD congruency with behavioral congruency
 372 gave a trend correlation for area 46; $r(38) = .31$, $p = .05$ and no correlation for FPM; $r(38) = .07$, $p =$
 373 $.63$. These correlations did not differ from the congruency-FPI correlation, both $p > .2$.

374

{Insert Figure 1}

Relation between AA-related activity and functional fingerprints of FPI (Resting-state connectivity)

To assess whether the aPFC activity evoked during emotional-action control falls within FPI (Neubert et al. 2014), we compared resting-state connectivity profiles of area 46, FPI and FPM with the connectivity profile of the aPFC clusters showing a congruency effect (MNI: [24 50 -4] and [-24 52 -4]). We tested whether the connectivity fingerprints of the three prefrontal areas differed from the connectivity profile of the AA-related clusters, figure 2.

Qualitative inspection of the resting-state fingerprints showed relatively similar connectivity profiles for area 46 and FPI. Both are strongly correlated with the intraparietal sulcus (IPI) and dorsolateral prefrontal cortex (dlPFC); however, FPI shows stronger connectivity to the posterior cingulate cortex (PCC). Functional connectivity of FPM differed quite strongly from both area 46 and FPI, showing strongest connectivity with ventromedial prefrontal areas (vmPFC), PCC and temporal pole (TP), figure 2A;C. These results corroborate earlier reports on resting-state connectivity fingerprints for these areas (Neubert et al., 2014; Mars et al., 2016; Hartogsveld et al., 2017).

Comparing connectivity profiles between the three areas in aPFC with the connectivity profile extracted from the AA-related region showed that its fingerprint differed significantly from that of area 46, (left hemisphere: $p < .001$; right-hemisphere: $p < .001$), and from that of area FPM (right hemisphere: $p < .001$; left-hemisphere: $p < .001$), but not from the connectivity fingerprint of area FPI (left-hemisphere: $p = .87$, right-hemisphere: $p = .075$). This result provides evidence that control of social emotional action-tendencies involves the lateral Frontal Pole.

Relation between AA-related activity and structural fingerprints of FPI (DWI connectivity)

In addition to resting-state connectivity, we created connectivity profiles based on white matter tractography. We placed seeds in five large white matter tracts (figure 2B); performed probabilistic tractography to the rest of the hemisphere; and counted how often each tract ended in

each of the three regions in aPFC (figure 2B). We used a similar procedure for amygdalofugal (AmF) connectivity (see methods).

Comparing connectivity profiles of the aPFC regions to these five major white matter tracts and AmF connectivity showed relatively strong connectivity between area 46 and the three superior longitudinal fasciculi (SLF1, SLF2 and SLF3; figure 2D). FPM is most strongly connected to the Cingulate Bundle, Uncinate Fasciculus and Amygdalofugal pathways. FPI is less strongly connected to the tracts leading outside the frontal cortex, and more strongly connected to the Uncinate Fasciculus, which leads to the temporal pole (among other regions). The AA-related regions are also more strongly connected to the Uncinate Fasciculus. These results are shown in figure 2D and match earlier reports on connectivity of aPFC regions (Neubert et al., 2014; Mars et al., 2016; Hartogsveld et al., 2017).

Comparing connectivity profiles between the three areas in aPFC with the connectivity profile extracted from the AA region showed that the fingerprint of the AA region differed significantly from that of area 46, (left hemisphere: $p < .001$; right-hemisphere: $p < .001$), and from that of area FPM (right hemisphere: $p < .001$; left-hemisphere: $p < .001$), but not from the connectivity fingerprint of area FPI (left-hemisphere: $p = .98$, right-hemisphere: $p = 1$). This result corroborates the resting state results, providing additional evidence that the FPI is one of the regions involved in controlling social emotional action-tendencies.

{Insert Figure 2}

FPI-amygdalofugal connectivity partly explains performance on the AA task.

421 To identify an anatomical pathway through which the FPI could support emotional behavior,
 422 we tested whether inter-subject variability in the strength of FPI structural connectivity mediated by
 423 the amygdalofugal connections predicts successful performance on the AA task. On average, the FPM
 424 is more strongly connected to amygdalofugal pathways than the FPI and area 46 (Figure 3A), in line
 425 with earlier studies showing both functionally and anatomically stronger connections between limbic
 426 areas and medial prefrontal regions (Ghashghaei and Barbas, 2002; Neubert et al., 2014; Folloni et
 427 al., 2019). However, individual variability in the connectivity of FPI and FPM confirms that the former
 428 region is more strongly involved in emotional action control than the latter. Namely, there was a
 429 significant correlation between tract strength and AA congruency effect on percentage correct;
 430 Spearman's $r(38) = .44$, $p = .004$ for the FPI connections but not for FPM, $r(38) = .24$, $p = .13$ and area
 431 46, $r(38) = .3$, $p = .062$, figure 3B. However, these correlations did not differ from one another, both
 432 comparisons $p > .3$. The direction of the FPI-behavioral correlation indicated that stronger
 433 connectivity was related to relatively worse performance when having to exert control. There were
 434 no significant correlations between tract strength and congruency effect on reaction time; all $p > .09$.
 435 The congruency-FPI correlation for percentage correct survives Bonferroni-correction for multiple
 436 comparisons over the eight correlations computed between behavioral congruency and
 437 amygdalofugal-FPI connectivity; and the two control correlations described below.

438 To facilitate data interpretation, we conducted 2 additional exploratory control analyses.
 439 First, to exclude that the correlation between amygdalofugal-FPI connectivity and AA performance
 440 could be better explained by connections between amygdala and FPI through the Uncinate Fasciculus
 441 (UF; Petrides and Pandya 2007) or trait anxiety (Kim and Whalen, 2009), we correlated UF-FPI
 442 connectivity with AA performance, and amygdalofugal-FPI connectivity with scores on the State
 443 anxiety inventory (STAI). None of these analyses yielded significant correlations, all $p > .58$. Nor did
 444 the correlation between amygdalofugal-FPI connections and behavioral congruency change when
 445 controlling for state anxiety or UF-FPI connectivity.

Second, to explore whether FPI-amygdalofugal connectivity would also influence functional connectivity between these two areas, we performed a Psychophysiological Interaction (PPI) analysis with bilateral amygdalae as seed region and the strength of the connection with FPI as covariate. This analysis showed a negative correlation between tract strength and amygdala-FPI functional connectivity during the task, when using a small volume correction over bilateral FPI; $p = .019$ (FWE cluster corrected; cluster location MNI [-32 50 6], cluster size: 20 voxels), meaning that with increased tract strength there is more negative connectivity between the FPI and amygdala, which might be interpreted as increased regulation of amygdala by the FPI (Volman et al., 2013).

Finally, given the novelty of the role of the amygdalofugal path in emotion control, we tested whether the correlation between behavioral congruency and amygdalofugal connectivity would replicate in an independent sample of 50 participants. The positive relationship between the congruency effect in % correct on the AA task and amygdalofugal-FPI connections was confirmed; Pearson's $r(48) = .3$, $p = .03$; Spearman's $r(48) = .28$, $p = .05$, figure 3C, further substantiating this finding.

460

{Insert Figure 3}

462

463 Discussion

The present study anatomically qualifies the involvement of the anterior prefrontal cortex in control of action-tendencies elicited by emotional faces. There are two main findings. First, structural and functional connectivity fingerprints of the lateral Frontal Pole (Neubert et al., 2014) closely match the fingerprints of the aPFC territory recruited when emotional action control is required. Second, the strength of FPI structural connectivity with the amygdala accounts for a substantial portion of inter-individual variation in emotional action regulation abilities. These findings provide

evidence for a precise cortical region (FPI) and a structural pathway (the ventral amygdalofugal bundle) through which a cognitively complex form of emotional regulation might be implemented in the human brain.

FPI supports emotional-action control

Previous work has repeatedly shown that the aPFC is involved in controlling emotional behavior, and that it is capable of doing so by influencing downstream activity in the amygdala (Volman et al. 2013; Tyborowska et al. 2016); motor cortex; and parietal areas (Volman et al. 2011; Bramson et al. 2018). Here, we extend this knowledge by showing that the aPFC contribution to emotional action control arises from a precise anatomical structure: the lateral Frontal Pole (Neubert et al., 2014). This finding is based on the connectivity fingerprint of the FPI. This anatomical metric also provides clues to the information received by the FPI, and the influence it can exert on other brain structures (Mars et al., 2018). The FPI, differently from neighbouring areas FPM and 46, is connected to both medial and lateral circuits with parietal, cingulate, and temporal regions (Figure 2). The peculiar pattern of FPI connectivity fits with the known supramodal regulatory role of this area during social-emotional control (Volman et al. 2011; Volman et al. 2013; Koch et al. in prep), and with the notion that social-emotional regulation involves access to both egocentric value of emotionally-laden actions, as well as social consequences of those actions (Koch et al., 2018).

This study was designed to add functional specificity to those anatomically-grounded inferences on aPFC contributions to emotional-action regulation. The observations of this study link emotional-action regulation to several cognitive processes that rely on the FPI, e.g. concurrent monitoring of current and alternative goals (Burgess et al., 2007; Badre and D'Esposito, 2009; Mansouri et al., 2017), cognitive exploration (Daw et al., 2006; Zajkowski et al., 2017), counterfactual reasoning (Boorman et al., 2009b; Koechlin, 2016), metacognition (Fleming et al., 2014; Shekhar and Rahnev, 2018), and relational reasoning (Vendetti and Bunge, 2014; Hartogsveld et al., 2017). More precisely, it becomes relevant to test whether the FPI contribution to emotional-action control is

495 linked to the online maintenance and evaluation of alternative goals or counterfactual regulation
 496 strategies (Sheppes et al., 2014; Koch et al., 2018); or whether the cognitive demands of emotional
 497 action control and their input-output connectivity segregate this faculty from other known FPI
 498 functions.

499 **Amygdala-FPI projections modulate control over emotional-action**

500 This study shows that control over emotional actions is negatively associated with the
 501 strength of amygdala-FPI connections, with connections between amygdala and FPI explaining
 502 between 10-20% of the variance on the AA task. This result was confirmed in an independent
 503 replication sample. On the assumption that the amygdala-FPI connectivity indexed in this study
 504 captures the amygdalofugal pathway (Folloni et al. 2019), i.e. the main efferent pathways from
 505 amygdala to frontal cortex (Nolte, 1999; Ghashghaei and Barbas, 2002; Noback et al., 2005; Krüger et
 506 al., 2015; Kamali et al., 2016), this finding suggests that stronger amygdala projections to the FPI
 507 impair emotional regulation. Namely, during incongruent trials, stronger amygdala afferences to the
 508 FPI could lead to stronger automatic action-tendencies or heightened emotional vigilance and thus
 509 more errors when those tendencies need to be rapidly over-ruled. This observation fits with previous
 510 imaging work showing that successful emotional control reduces bottom-up effective connectivity
 511 between amygdala and aPFC (Volman et al., 2013). Moreover, it suggests that top-down regulatory
 512 FPI efferences might reach the amygdala through other fiber bundles, e.g. the uncinate fasciculus
 513 (Petrides and Pandya, 2007; Folloni et al., 2019); or through other regions, e.g. the nucleus
 514 accumbens (Wager et al., 2008) or the orbitofrontal cortex (Ray and Zald, 2012).

515 The relation between amygdala-FPI connectivity strength and emotional action control
 516 observed in this study is surprisingly large when compared to the magnitude of previous structure-
 517 function correlations in the same anatomical regions (Jung et al., 2018). We suspect that the large
 518 effect size is a consequence of considering the anatomical differences between fiber bundles
 519 connecting the amygdala to the prefrontal cortex, and in particular the uniquely human configuration

520 of that connectivity, since anthropoid monkeys do not possess a functional homologue of the human
 521 lateral Frontal Pole (Semendeferi et al., 2010; Neubert et al., 2014; Mars et al., 2016). Future tests of
 522 this potential functional-anatomical dissociation between bottom-up and top-down amygdala-FPI
 523 connectivity might also help to clarify the heterogeneity of previous findings concerning the relation
 524 between amygdala-prefrontal connectivity and state-anxiety measures (Kim and Whalen, 2009;
 525 Clewett et al., 2014).

526 **Interpretational issues**

527 It could be argued that the regulation required in the AA task is just an instance of inhibitory
 528 control with social stimuli, and that regulation in this task could be accomplished by suppressing
 529 automatic emotional action-tendencies (Etkin et al., 2006; Aron et al., 2014). Several studies have
 530 shown that this is not a viable option. First, when participants respond to the gender rather than the
 531 emotion of the face, both behavioral (congruency effect) and neural correlates of emotional control
 532 (FPI activation) are extinguished (Roelofs et al., 2008; Volman et al., 2011b). This illustrates that the
 533 regulation indexed by the AA task crucially depends on the interaction between emotional percepts
 534 and action selection, rather than on overriding conflict contained in the stimulus itself (e.g.
 535 emotional Stroop task, which is supported by different neural circuitry (Etkin et al., 2011, 2015)).
 536 Second, performance on the AA task is specifically altered in patients with disrupted social-emotional
 537 regulation (Heuer et al., 2007; van Peer et al., 2009; von Borries et al., 2012). For instance,
 538 aggression-related psychopathologies such as psychopathy are marked by reduction of avoidance
 539 responses, specific to angry faces, an effect related to measures of social aggression (von Borries et
 540 al., 2012). In contrast, patients with social anxiety disorder show a consistent increase of avoidance
 541 responses, specific to angry faces (Roelofs et al., 2005, 2009, 2010; Heuer et al., 2007). In addition,
 542 socially-relevant hormones such as testosterone (Tyborowska et al., 2016), cortisol (Volman et al.,
 543 2011b), and oxytocin (Radke et al., 2017) influence performance of the Approach-Avoidance task in
 544 healthy participants. Most critically, the aPFC congruency effect measured during the social

545 approach-avoidance task is predictive of subjective, physiological and hormonal responses to a real-
 546 life social stressor (Kaldewaij et al., 2019b). In sum, these studies highlight the validity of the AA task
 547 for indexing regulation of emotional actions in social contexts.

548 In principle, the relation between strength of amygdala-FPI connectivity and behavioral
 549 emotional control could be explained by a third factor, e.g. trait anxiety. However, the tract strength
 550 between amygdala and FPI did not correlate with trait anxiety, and the correlation between
 551 behavioral congruency and tract strength persisted when controlling for anxiety. This observation
 552 confirms that, in healthy participants, aPFC activity during the AA task is orthogonal to trait anxiety
 553 effects (Bramson et al., 2018), in contrast to known trait anxiety effects on amygdala-vmPFC
 554 connectivity (Kim and Whalen, 2009).

555 It is not easy to acquire reliable fMRI signals from anterior prefrontal regions (Hutton et al.,
 556 2002). Therefore, we used magnetic field corrections to restore signal distortions around the frontal
 557 pole (Jezzard and Balaban, 1995; Jenkinson, 2004). The resting-state connectivity profiles closely
 558 matched those of earlier studies that used different MRI protocols (Neubert et al., 2014; Mars et al.,
 559 2016) arguing against the possibility that the results reported here can be attributed to signal
 560 distortions. The first sample of participants consisted of males only, and the replication sample was
 561 predominantly male. Whereas behavioral and neural effects in the AA task have been shown in
 562 mixed and female only samples as well (Radke et al., 2015; Tyborowska et al., 2016; Bertsch et al.,
 563 2018), we recruited only males to avoid having to control for differences in social hormones such as
 564 testosterone and cortisol, which would require a larger sample of participants. These hormones are
 565 known to influence behavioral and neural responses on the AA task (van Peer et al., 2007; Volman et
 566 al., 2011b; Kaldewaij et al., 2019a). Future studies could explore similarities and potential differences
 567 in emotional processing between sexes (Domes et al., 2010; Whittle et al., 2011).

568 **Conclusion**

569 This study provides anatomical evidence supporting the involvement of the lateral frontal
 570 pole, partly via the ventral amygdalofugal pathway, in the regulation of emotional behavior (Koch et
 571 al., 2018). The findings have implications for structuring mechanism-based interventions in
 572 psychopathologies characterized by altered emotional control abilities, e.g. anxiety disorders and
 573 psychopathy (Volman et al., 2016). The findings are also relevant for understanding the
 574 neurobiological and cognitive complexities underlying rule-based regulation of action-tendencies,
 575 arguably a crucial pre-requisite for the development of human cumulative culture (Hare, 2017;
 576 Whiten, 2017).

577

578 References

- 579 Andersson JLR, Skare S, Ashburner J (2003) How to correct susceptibility distortions in spin-echo
 580 echo-planar images: application to diffusion tensor imaging. *Neuroimage* 20:870–888.
- 581 Andersson JLR, Sotiropoulos SN (2016) An integrated approach to correction for off-resonance
 582 effects and subject movement in diffusion MR imaging. *Neuroimage* 125:1063–1078.
- 583 Aron AR, Robbins TW, Poldrack RA (2014) Inhibition and the right inferior frontal cortex: one decade
 584 on. *Trends Cogn Sci* 18:177–185.
- 585 Badre D, D’esposito M (2009) Is the rostro-caudal axis of the frontal lobe hierarchical? *Nat Rev*
 586 *Neurosci* 10:659–669.
- 587 Beckmann CF, Smith SM (2004) Probabilistic independent component analysis for functional
 588 magnetic resonance imaging. *IEEE Trans Med Imaging* 23:137–152.
- 589 Behrens TEJ, Berg HJ, Jbabdi S, Rushworth MFS, Woolrich MW (2007) Probabilistic diffusion
 590 tractography with multiple fibre orientations: What can we gain? *Neuroimage* 34:144–155.
- 591 Bertsch K, Roelofs K, Roch PJ, Ma B, Hensel S, Herpertz SC, Volman I (2018) Neural correlates of

- 592 emotional action control in anger-prone women with borderline personality disorder. J
593 psychiatry Neurosci JPN 43:170102.
- 594 Bertsch K, Volman I, Roelofs K, Herpertz SC, Müller LE (2017) Social emotional leaning and behavioral
595 tendencies in high and low socially anxious men and women. Psychoneuroendocrinology 83:49.
- 596 Boorman ED, Behrens TEJ, Woolrich MW, Rushworth MFS (2009a) How Green Is the Grass on the
597 Other Side? Frontopolar Cortex and the Evidence in Favor of Alternative Courses of Action.
598 Neuron 62:733–743 Available at: <http://dx.doi.org/10.1016/j.neuron.2009.05.014>.
- 599 Boorman ED, Behrens TEJ, Woolrich MW, Rushworth MFS (2009b) How green is the grass on the
600 other side? Frontopolar cortex and the evidence in favor of alternative courses of action.
601 Neuron 62:733–743.
- 602 Bramson B, Jensen O, Toni I, Roelofs K (2018) Cortical oscillatory mechanisms supporting the control
603 of human social-emotional actions. J Neurosci:3317–3382.
- 604 Buhle JT, Silvers JA, Wager TD, Lopez R, Onyemekwu C, Kober H, Weber J, Ochsner KN (2014)
605 Cognitive reappraisal of emotion: a meta-analysis of human neuroimaging studies. Cereb cortex
606 24:2981–2990.
- 607 Burgess PW, Dumontheil I, Gilbert SJ (2007) The gateway hypothesis of rostral prefrontal cortex (area
608 10) function. Trends Cogn Sci 11:290–298.
- 609 Daw ND, O’doherly JP, Dayan P, Seymour B, Dolan RJ (2006) Cortical substrates for exploratory
610 decisions in humans. Nature 441:876–879.
- 611 Domes G, Schulze L, Böttger M, Grossmann A, Hauenstein K, Wirtz PH, Heinrichs M, Herpertz SC
612 (2010) The neural correlates of sex differences in emotional reactivity and emotion regulation.
613 Hum Brain Mapp 31:758–769.
- 614 Eklund A, Nichols T, Knutsson H (2015) Can parametric statistical methods be trusted for fMRI based

- group studies? *Proc Natl Acad Sci* 113:7900–7905 Available at:
<http://arxiv.org/abs/1511.01863> <http://dx.doi.org/10.1073/pnas.1602413113>.
- Etkin A, Büchel C, Gross JJ (2015) The neural bases of emotion regulation. *Nat Rev Neurosci* 16:693.
- Etkin A, Egner T, Kalisch R (2011) Emotional processing in anterior cingulate and medial prefrontal cortex. *Trends Cogn Sci* 15:85–93.
- Etkin A, Egner T, Peraza DM, Kandel ER, Hirsch J (2006) Resolving emotional conflict: a role for the rostral anterior cingulate cortex in modulating activity in the amygdala. *Neuron* 51:871–882.
- Fleming SM, Ryu J, Golfinos JG, Blackmon KE (2014) Domain-specific impairment in metacognitive accuracy following anterior prefrontal lesions. *Brain* 137:2811–2822.
- Folloni D, Sallet J, Khrapitchev AA, Sibson N, Verhagen L, Mars RB (2019) Dichotomous organization of amygdala/temporal-prefrontal bundles in both humans and monkeys Heilbronner S, Gold JI, Thiebaut de Schotten M, eds. *Elife* 8:e47175.
- Frijda NH, Ridderinkhof KR, Rietveld E (2014) Impulsive action: emotional impulses and their control. *Front Psychol* 5:518.
- Ghashghaei HT, Barbas H (2002) Pathways for emotion: interactions of prefrontal and anterior temporal pathways in the amygdala of the rhesus monkey. *Neuroscience* 115:1261–1279.
- Ghashghaei HT, Hilgetag CC, Barbas H (2007) Sequence of information processing for emotions based on the anatomic dialogue between prefrontal cortex and amygdala. *Neuroimage* 34:905–923.
- Griffanti L, Douaud G, Bijsterbosch J, Evangelisti S, Alfaro-Almagro F, Glasser MF, Duff EP, Fitzgibbon S, Westphal R, Carone D (2017) Hand classification of fMRI ICA noise components. *Neuroimage* 154:188–205.
- Hare B (2017) Survival of the friendliest: *Homo sapiens* evolved via selection for prosociality. *Annu*

- 637 Rev Psychol 68:155–186.
- 638 Hartogsveld B, Bramson B, Vijayakumar S, van Campen AD, Marques JP, Roelofs K, Toni I, Bekkering
639 H, Mars RB (2017) Lateral frontal pole and relational processing: Activation patterns and
640 connectivity profile. Behav Brain Res.
- 641 Heuer K, Rinck M, Becker ES (2007) Avoidance of emotional facial expressions in social anxiety: The
642 Approach–Avoidance Task. Behav Res Ther 45:2990–3001.
- 643 Hutton C, Bork A, Josephs O, Deichmann R, Ashburner J, Turner R (2002) Image distortion correction
644 in fMRI: a quantitative evaluation. Neuroimage 16:217–240.
- 645 Jenkinson M (2004) Improving the registration of B0-distorted EPI images using calculated cost
646 function weights. In: Tenth International Conference on functional mapping of the human brain.
- 647 Jenkinson M, Bannister P, Brady M, Smith S (2002) Improved optimization for the robust and
648 accurate linear registration and motion correction of brain images. Neuroimage 17:825–841.
- 649 Jezzard P, Balaban RS (1995) Correction for geometric distortion in echo planar images from B0 field
650 variations. Magn Reson Med 34:65–73.
- 651 Kaldewaij R, Koch SBJ, Zhang W, Hashemi MM, Klumpers F, Roelofs K (2019a) High endogenous
652 testosterone levels are associated with diminished neural emotional control in aggressive police
653 recruits. Psychol Sci:0956797619851753.
- 654 Kaldewaij R, Koch SBJ, Zhang W, Hashemi MM, Klumpers F, Roelofs K (2019b) Frontal control over
655 automatic emotional action tendencies predicts acute stress responsivity. Biol Psychiatry Cogn
656 Neurosci Neuroimaging.
- 657 Kamali A, Sair HI, Blitz AM, Riascos RF, Mirbagheri S, Keser Z, Hasan KM (2016) Revealing the ventral
658 amygdalofugal pathway of the human limbic system using high spatial resolution diffusion
659 tensor tractography. Brain Struct Funct 221:3561–3569.

- 660 Kim MJ, Whalen PJ (2009) The structural integrity of an amygdala–prefrontal pathway predicts trait
661 anxiety. *J Neurosci* 29:11614–11618.
- 662 Koch SBJ, Mars RB, Toni I, Roelofs K (2018) Emotional control, reappraised. *Neurosci Biobehav Rev*
663 95:528–534 Available at: <https://linkinghub.elsevier.com/retrieve/pii/S0149763418301672>.
- 664 Koechlin E (2016) Prefrontal executive function and adaptive behavior in complex environments. *Curr*
665 *Opin Neurobiol* 37:1–6.
- 666 Krüger O, Shiozawa T, Kreifelts B, Scheffler K, Ethofer T (2015) Three distinct fiber pathways of the
667 bed nucleus of the stria terminalis to the amygdala and prefrontal cortex. *Cortex* 66:60–68.
- 668 Langner R, Leiberg S, Hoffstaedter F, Eickhoff SB (2018) Towards a human self-regulation system:
669 Common and distinct neural signatures of emotional and behavioural control. *Neurosci*
670 *Biobehav Rev* 90:400–410.
- 671 Mansouri FA, Koechlin E, Rosa MGP, Buckley MJ (2017) Managing competing goals—a key role for the
672 frontopolar cortex. *Nat Rev Neurosci*.
- 673 Mars RB, Jbabdi S, Sallet J, O'Reilly JX, Croxson PL, Olivier E, Noonan MP, Bergmann C, Mitchell AS,
674 Baxter MG (2011) Diffusion-weighted imaging tractography-based parcellation of the human
675 parietal cortex and comparison with human and macaque resting-state functional connectivity.
676 *J Neurosci* 31:4087–4100.
- 677 Mars RB, Passingham RE, Jbabdi S (2018) Connectivity Fingerprints: From Areal Descriptions to
678 Abstract Spaces. *Trends Cogn Sci* 22:1026–1037 Available at:
679 <https://doi.org/10.1016/j.tics.2018.08.009>.
- 680 Mars RB, Verhagen L, Gladwin TE, Neubert F-X, Sallet J, Rushworth MFS (2016) Comparing brains by
681 matching connectivity profiles. *Neurosci Biobehav Rev* 60:90–97.
- 682 Morawetz C, Bode S, Derntl B, Heekeren HR (2017) The effect of strategies, goals and stimulus

- 683 material on the neural mechanisms of emotion regulation: A meta-analysis of fMRI studies.
 684 *Neurosci Biobehav Rev* 72:111–128 Available at:
 685 <http://www.sciencedirect.com/science/article/pii/S014976341630375X> [Accessed June 22,
 686 2017].
- 687 Motzkin JC, Philippi CL, Wolf RC, Baskaya MK, Koenigs M (2015) Ventromedial prefrontal cortex is
 688 critical for the regulation of amygdala activity in humans. *Biol Psychiatry* 77:276–284.
- 689 Neubert F-X, Mars RB, Thomas AG, Sallet J, Rushworth MFS (2014) Comparison of human ventral
 690 frontal cortex areas for cognitive control and language with areas in monkey frontal cortex.
 691 *Neuron* 81:700–713.
- 692 Noback CR, Ruggiero DA, Demarest RJ, Strominger NL (2005) The human nervous system: structure
 693 and function. Springer Science & Business Media.
- 694 Nolte J (1999) The human brain: an introduction to its functional anatomy. Mosby Inc.
- 695 Passingham RE, Stephan KE, Kötter R (2002) The anatomical basis of functional localization in the
 696 cortex. *Nat Rev Neurosci* 3:606.
- 697 Petrides M, Pandya DN (2007) Efferent association pathways from the rostral prefrontal cortex in the
 698 macaque monkey. *J Neurosci* 27:11573–11586.
- 699 Radke S, Roelofs K, De Bruijn ERA (2013) Acting on anger: social anxiety modulates approach-
 700 avoidance tendencies after oxytocin administration. *Psychol Sci* 24:1573–1578.
- 701 Radke S, Volman I, Kokal I, Roelofs K, de Bruijn ERA, Toni I (2017) Oxytocin reduces amygdala
 702 responses during threat approach. *Psychoneuroendocrinology* 79:160–166.
- 703 Radke S, Volman I, Mehta P, van Son V, Enter D, Sanfey A, Toni I, de Bruijn ERA, Roelofs K (2015)
 704 Testosterone biases the amygdala toward social threat approach. *Sci Adv* 1:e1400074.

- 705 Ramnani N, Owen AM (2004) Anterior prefrontal cortex: insights into function from anatomy and
706 neuroimaging. *Nat Rev Neurosci* 5.
- 707 Ray RD, Zald DH (2012) Anatomical insights into the interaction of emotion and cognition in the
708 prefrontal cortex. *Neurosci Biobehav Rev* 36:479–501.
- 709 Ridderinkhof KR (2017) Emotion in action: A predictive processing perspective and theoretical
710 synthesis. *Emot Rev* 9:319–325.
- 711 Roelofs K, Cremers HR (2015) Cortical-amygdala decoupling during stress in patients with social
712 anxiety disorder. *Biol Psychiatry* 77:S298–S298.
- 713 Roelofs K, Minelli A, Mars RB, Van Peer J, Toni I (2008) On the neural control of social emotional
714 behavior. *Soc Cogn Affect Neurosci*:nsn036.
- 715 Roelofs K, van Peer J, Berretty E, de Jong P, Spinhoven P, Elzinga BM (2009) Hypothalamus–pituitary–
716 adrenal axis hyperresponsiveness is associated with increased social avoidance behavior in
717 social phobia. *Biol Psychiatry* 65:336–343.
- 718 Sallet J, Mars RB, Noonan MP, Neubert F-X, Jbabdi S, O’Reilly JX, Filippini N, Thomas AG, Rushworth
719 MF (2013) The organization of dorsal frontal cortex in humans and macaques. *J Neurosci*
720 33:12255–12274.
- 721 Semendeferi K, Teffer K, Buxhoeveden DP, Park MS, Bludau S, Amunts K, Travis K, Buckwalter J (2010)
722 Spatial organization of neurons in the frontal pole sets humans apart from great apes. *Cereb*
723 *cortex* 21:1485–1497.
- 724 Shekhar M, Rahnev D (2018) Distinguishing the Roles of Dorsolateral and Anterior PFC in Visual
725 Metacognition. *J Neurosci* 38:5078–5087 Available at:
726 <http://www.jneurosci.org/lookup/doi/10.1523/JNEUROSCI.3484-17.2018>.
- 727 Sheppes G, Scheibe S, Suri G, Radu P, Blechert J, Gross JJ (2014) Emotion regulation choice: a

- conceptual framework and supporting evidence. *J Exp Psychol Gen* 143:163.
- Tillman RM, Stockbridge MD, Nacewicz BM, Torrisi S, Fox AS, Smith JF, Shackman AJ (2018) Intrinsic functional connectivity of the central extended amygdala. *Hum Brain Mapp* 39:1291–1312.
- Tyborowska A, Volman I, Smeekens S, Toni I, Roelofs K (2016) Testosterone during puberty shifts emotional control from pulvinar to anterior prefrontal cortex. *J Neurosci* 36:6156–6164.
- Tzourio-Mazoyer N, Landeau B, Papathanassiou D, Crivello F, Etard O, Delcroix N, Mazoyer B, Joliot M (2002) Automated anatomical labeling of activations in SPM using a macroscopic anatomical parcellation of the MNI MRI single-subject brain. *Neuroimage* 15:273–289.
- van Peer JM, Roelofs K, Rotteveel M, van Dijk JG, Spinhoven P, Ridderinkhof KR (2007) The effects of cortisol administration on approach–avoidance behavior: an event-related potential study. *Biol Psychol* 76:135–146.
- van Peer JM, Spinhoven P, van Dijk JG, Roelofs K (2009) Cortisol-induced enhancement of emotional face processing in social phobia depends on symptom severity and motivational context. *Biol Psychol* 81:123–130.
- Vendetti MS, Bunge SA (2014) Evolutionary and Developmental Changes in the Lateral Frontoparietal Network: A Little Goes a Long Way for Higher-Level Cognition. *Neuron* 84:906–917 Available at: <http://www.ncbi.nlm.nih.gov/pmc/articles/PMC4527542/>.
- Volman I, Roelofs K, Koch S, Verhagen L, Toni I (2011a) Anterior prefrontal cortex inhibition impairs control over social emotional actions. *Curr Biol* 21:1766–1770.
- Volman I, Toni I, Verhagen L, Roelofs K (2011b) Endogenous testosterone modulates prefrontal–amygdala connectivity during social emotional behavior. *Cereb Cortex*:bhr001.
- Volman I, Verhagen L, den Ouden HEM, Fernández G, Rijpkema M, Franke B, Toni I, Roelofs K (2013) Reduced serotonin transporter availability decreases prefrontal control of the amygdala. *J*

- 751 Neurosci 33:8974–8979.
- 752 Volman I, von Borries AKL, Bulten BH, Verkes RJ, Toni I, Roelofs K (2016) Testosterone modulates
753 altered prefrontal control of emotional actions in psychopathic offenders. *ENeuro* 3:ENEURO-
754 0107.
- 755 von Borries AKL, Volman I, de Bruijn ERA, Bulten BH, Verkes RJ, Roelofs K (2012) Psychopaths lack the
756 automatic avoidance of social threat: relation to instrumental aggression. *Psychiatry Res*
757 200:761–766.
- 758 Wager TD, Davidson ML, Hughes BL, Lindquist MA, Ochsner KN (2008) Prefrontal-subcortical
759 pathways mediating successful emotion regulation. *Neuron* 59:1037–1050.
- 760 Whiten A (2017) Culture extends the scope of evolutionary biology in the great apes. *Proc Natl Acad*
761 Sci 114:7790–7797 Available at: <http://www.pnas.org/lookup/doi/10.1073/pnas.1620733114>.
- 762 Whittle S, Yücel M, Yap MBH, Allen NB (2011) Sex differences in the neural correlates of emotion:
763 evidence from neuroimaging. *Biol Psychol* 87:319–333.
- 764 Woolrich MW, Behrens TEJ, Beckmann CF, Jenkinson M, Smith SM (2004) Multilevel linear modelling
765 for FMRI group analysis using Bayesian inference. *Neuroimage* 21:1732–1747 Available at:
766 <http://www.sciencedirect.com/science/article/pii/S1053811903007894>.
- 767 Woolrich MW, Ripley BD, Brady M, Smith SM (2001) Temporal Autocorrelation in Univariate Linear
768 Modeling of FMRI Data. *Neuroimage* 14:1370–1386 Available at:
769 <http://www.sciencedirect.com/science/article/pii/S1053811901909310>.
- 770 Zajkowski WK, Kossut M, Wilson RC (2017) A causal role for right frontopolar cortex in directed, but
771 not random, exploration. *Elife* 6.
- 772

773 **Figure legends**

774 **Figure 1: Effects of cognitive control over social-emotional action tendencies.**

775 A) Schematic representation of the AA task used to measure control over social-emotional action
 776 tendencies. The incongruent condition requires control to override the automatic tendencies to
 777 approach happy- and avoid angry faces. B) Behavioral effects on AA task; participants show longer
 778 reaction times and more errors during the incongruent condition, illustrating the cost of exerting
 779 control. C) Main task effects for incongruent > congruent, masked to show above threshold (cluster
 780 level $p < .001$) activation in the anterior Prefrontal Cortex. (Frontal Pole mask; Harvard-oxford atlas)
 781 D) Correlation between reaction time congruency and BOLD congruency effects extracted from the
 782 lateral Frontal Pole across participants.

783 **Figure 2: AA task effects are localized within the connectivity-defined lateral Frontal Pole.**

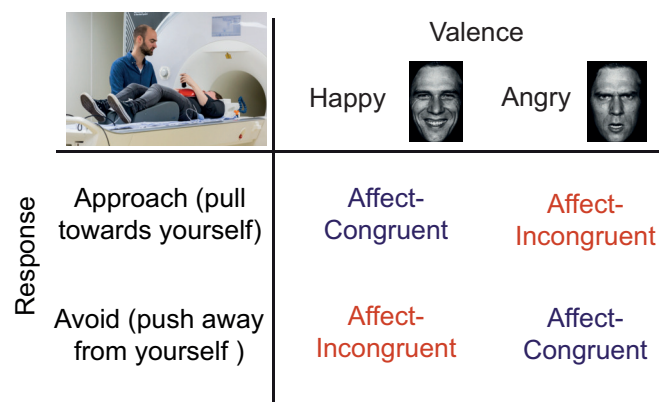
784 A) Seed regions and whole brain resting-state connectivity for area 46, FPM, FPI, and for the cluster
 785 showing AA task-effects. B) Seed locations for tractography in five large white matter tracts (AmF
 786 seed not shown) and masks for the regions FPI, FPM and area 46. C) Resting state connectivity
 787 fingerprints of the aPFC and AA regions, separated for left and right ROI's. Region labels: Posterior
 788 Cingulate Cortex (PCC), ventromedial prefrontal cortex (vmPFC), Intraparietal Lobule (IPL),
 789 dorsolateral Prefrontal Cortex (dlPFC), Temporal Pole (TP). D) Connectivity fingerprints for
 790 tractography of aPFC and the AA regions, separated for left and right ROI's. Tract abbreviations:
 791 Superior Longitudinal Fasciculus (SLF1, SLF2, SLF3); Uncinate Fasciculus (UF); Cingulum Bundle (CB);
 792 Amygdalofugal (AmF).

793 **Figure 3: Amygdalofugal connections with FPI correlate with AA task performance.**

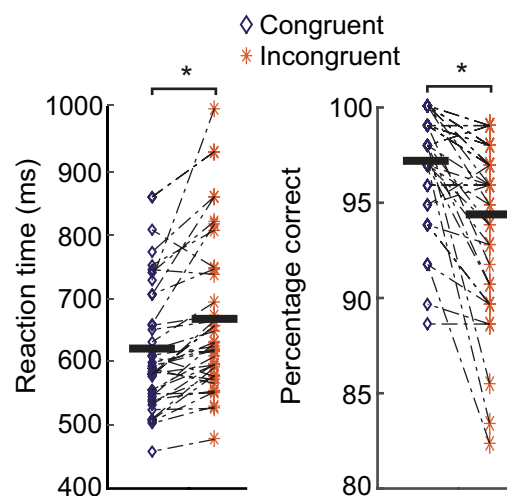
794 A) Illustration of the reconstructed tract that leads from the Amygdala to the anterior Prefrontal
 795 cortex. This tract shows strongest connectivity with medial prefrontal areas, as can be expected given
 796 earlier studies. B) The number of times the tract ends in FPI correlates with behavioral congruency in

797 error rates on the AA task, $r = .44$, $p = .0044$, suggesting that the amygdalofugal pathway is involved
798 in mediating FPI-amygdala functional interactions during social-emotional control. C) Illustration of
799 the reconstructed tract and correlation between behavioral congruency and tract strength with FPI in
800 the replication sample.

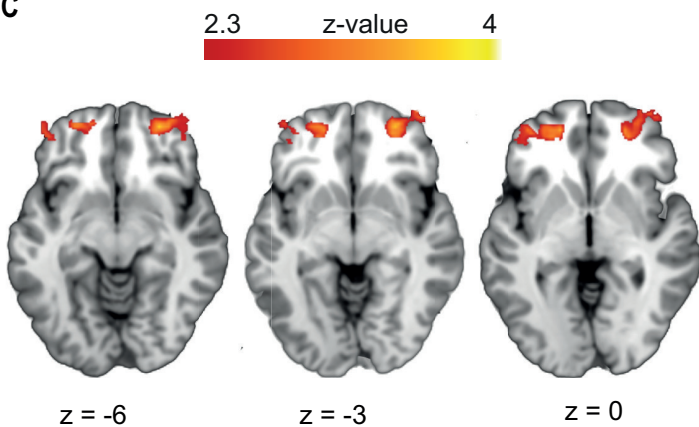
A



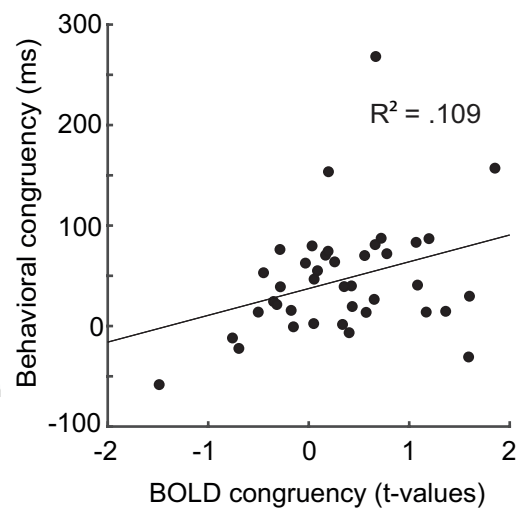
B



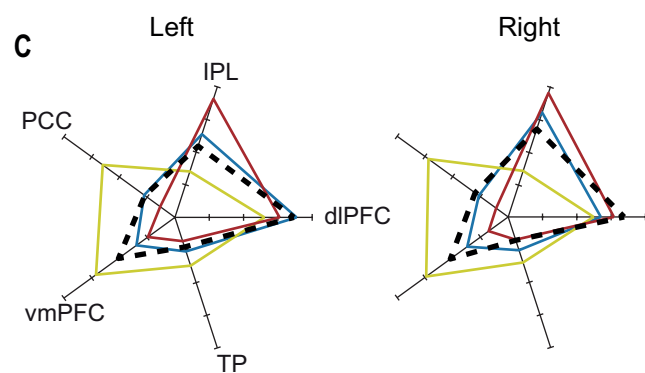
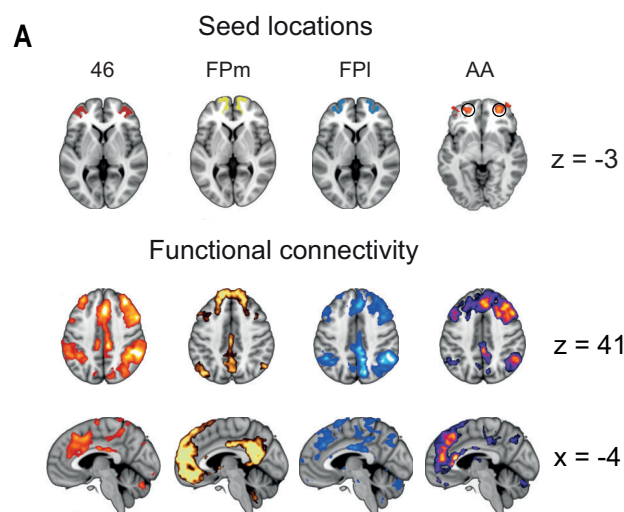
C



D



Resting state connectivity



Diffusion weighted connectivity

